

# Ballistic electronic transport in Quantum Cables

Z. Y. Zeng<sup>‡</sup>, Y. Xiang, and L. D. Zhang

*Institute of Solid State Physics, Chinese Academy of Sciences, P.O. Box 1129, Hefei,  
230031, P. R. China*

## Abstract

We studied theoretically ballistic electronic transport in a proposed mesoscopic structure - Quantum Cable. Our results demonstrated that Quantum Cable is a unique structure for the study of mesoscopic transport. As a function of Fermi energy, Ballistic conductance exhibits interesting stepwise features. Besides the steps of one or two quantum conductance units ( $2e^2/h$ ), conductance plateaus of more than two quantum conductance units can also be expected due to the accidental degeneracies (crossings) of subbands. As structure parameters is varied, conductance width displays oscillatory properties arising from the inhomogeneous variation of energy difference between adjoining transverse subbands. In the weak coupling limits, conductance steps of height  $2e^2/h$  becomes the first and second plateaus for the Quantum Cable of two cylinder wires with the same width.

**PACS** numbers: 73.23.Ad, 73.23.-b, 73.50.-h

## I. INTRODUCTION

Early investigations of ballistic electronic transport through microconstrictions led to the discovery of conductance quantization. Initially this phenomenon was observed in two-dimensional electron gas (2DEG) systems, manifesting itself in  $2e^2/h$  steplike variations of the conductance as a function of the transverse size of the narrowing<sup>1</sup>. It originates from the discrete character of propagating modes through the constriction due to the quantization of the transverse momentum. Under appropriate conditions, this phenomenon of conductance quantization should also occur in 3D point contacts with small constriction diameters<sup>2</sup>. Ballistic electron transport through narrow constrictions of different confining potential<sup>3</sup> has been extensively studied based on Landauer and Büttiker approach<sup>4</sup>. For a long constriction (quantum wire or quantum waveguide), ballistic conductance is directly proportional to the interger number of propagating modes or conductance channels and increases with the constriction width or Fermi energy in steps of  $2e^2/h$  each time a new channel opens up.

Owing to the recent advances in modern nanotechnologies, such as molecular-beam epitaxy, electron-beam lithography, self-assembled growth etc. , it has been possible to design and fabricate various kinds of mesoscopic devices<sup>5</sup>, in which electron can retain phase coherence while traveling through the active region. Successful experimental demonstration of mesoscopic devices have stimulated in turn much theoretical interest in exploiting the wave nature of electrons<sup>5,6</sup>. Mesoscopic devices are different from traditional electron devices in principle. In analyzing and designing mesoscopic quantum devices, it is essential to take into account the quantum character of electrons. Many kinds of quantum devices with various functions have been proposed and designed<sup>5,6</sup>. Research on these mesoscopic structures revealed many phenomena such as the quantized conductance of point contacts, persistent current through mesoscopic metallic ring, universal conductance fluctuations, Coulomb blockade, resonant tunneling, etc.<sup>7</sup> In particular, propagation of electrons along quantum wires of various geometries has been considered extensively<sup>8</sup>. More recently, del Alamo and Eugster have proposed and fabricated a new kind of mesoscopic device-coupled dual 2D quantum wires (2D CDQW) structure as field-effect directional couplers<sup>9</sup>. The operation principle of this device is based on the tunneling effects between electron waves propagating in the two adjacent waveguides through a controllable potential barrier. Later some groups<sup>10</sup> investigated its ballistic electronic transport

properties with and without the application of magnetic field.

A new kind of nanostructure referred to as Coaxial Nanocable has been successfully synthesized by Suenaga et al.<sup>11</sup> in 1997 and by Zhang et al.<sup>12</sup> in 1998. It comprises a solid and a hollow conducting cylinders of mesoscopic size separated by a insulating layer. If this insulating layer is not thick enough to forbid electrons' tunneling, it can be viewed as a coupled mesoscopic structure formed by two 3D quantum wires and a cylindrical potential barrier. This inspired us to propose a similar mesoscopic structure, Quantum Cable<sup>13</sup>, in which electron are confined in a Nanocable-like composite potential wells; i.e., electrons in the inner wire are subjected to a solid cylinder potential well, while electrons in the outer wire are limited into a hollow cylinder well; and they can tunnel into each other wire through the cylindrical coupling barrier. The structure of Quantum Cable is schematically shown in Fig. 1. Our previous calculations<sup>13</sup> showed that Quantum Cable has particular energy subband spectrum different from the 2D CDQW. For ballistic conductance, it is believed that there exists some significant discrepancies between the 2D and 3D quantum wire<sup>14</sup>. Therefore we expect Quantum Cable will exhibit unique transport properties, which are unexpected in the usual 2D CDQW structures.

The paper is organized as follows. In Section II, we present the formulas for calculating the ballistic conductance from Landauer and Büttiker's formula. Section III gives numerical calculations for ballistic conductances in some cases. We summarize our results in Section IV.

## II. MODEL AND FORMULATION

We consider ballistic electronic transport through the Quantum Cable structure between two large bulk reservoirs. The Quantum Cable comprises two coaxial cylindrical quantum wires - the inner wire is a solid cylinder well with radius  $R_1$  and the outer a hollow cylinder well with inner radius  $R_2$  and outer radius  $R_3$ . Two cylindrical wires are coupled through a thin layer of potential barrier of width  $R_B = R_2 - R_1$  and height  $U_B$ . The electrons are free to move along the  $z$  axis of Quantum Cable, whereas their motion in the radial direction is quantized. The cable length  $L$  is assumed to be, on the one hand, small compared to the elastic and inelastic mean free paths of the electrons (ballistic limit), and, on the other hand, large compared to the normal coherence length to ensure the absence of backscattering effects. Then the ballistic conductance of the Quantum Cable,

$G$ , is determined by the Landauer-Büttiker formula<sup>4</sup>

$$G = \frac{2e^2}{h} \sum T_{nl;n'l'}, \quad (1)$$

where  $T_{nl;n'l'}$  is the transmission probability of electrons from the incident transverse mode  $(n, l)$  to the outgoing mode  $(n', l')$ . The sum extends over all possible channels. If the applied contacts is adiabatic (i.e., whose dimensions changes slowly on the scale of the Fermi wavelength), and electron scattering in the contact regions is very weak, then the mode mixing can be neglected ( $T_{nl;n'l'} = 0$  if  $n \neq n'$  or  $l \neq l'$ ) and the transmission into the same channel  $T_{nl,nl} = 1$ . This allows us to express the conductance at low temperature as

$$G = \frac{2e^2}{h} \sum_{n,l} \Theta(E_F - E_{nl}), \quad (2)$$

where  $E_F$  is the Fermi energy and  $E_{nl}$  is the transverse part of the electron energy in Quantum Cable, which satisfies the follow relation derived from the standard effective-mass boundary conditions

$$F_1(k_2, k_3; R_1, R_2, R_3) + \frac{m_3^* k_2}{m_2^* k_3} F_2(k_2, k_3; R_1, R_2, R_3) + \frac{m_2^* k_1}{m_1^* k_2} \frac{J'_n(k_1 R_1)}{J_n(k_1 R_1)} \times \\ [G_1(k_2, k_3; R_1, R_2, R_3) + \frac{m_3^* k_2}{m_2^* k_3} G_2(k_2, k_3; R_1, R_2, R_3)] = 0, \quad (3)$$

where

$$F_1(k_2, k_3; R_1, R_2, R_3) = [K_n(k_2 R_2) I'_n(k_2 R_1) - K'_n(k_2 R_1) I_n(k_2 R_2)] \times \\ [J_n(k_3 R_3) Y'_n(k_3 R_2) - J'_n(k_3 R_2) Y_n(k_3 R_3)], \\ F_2(k_2, k_3; R_1, R_2, R_3) = [K'_n(k_2 R_1) I'_n(k_2 R_2) - K'_n(k_2 R_1) I'_n(k_2 R_2)] \times \\ [J_n(k_3 R_3) Y_n(k_3 R_2) - J_n(k_3 R_2) Y_n(k_3 R_3)], \\ G_1(k_2, k_3; R_1, R_2, R_3) = [K_n(k_2 R_1) I_n(k_2 R_2) - K_n(k_2 R_2) I_n(k_2 R_1)] \times \\ [J_n(k_3 R_3) Y'_n(k_3 R_2) - J'_n(k_3 R_2) Y_n(k_3 R_3)], \\ G_2(k_2, k_3; R_1, R_2, R_3) = [K'_n(k_2 R_2) I_n(k_2 R_1) - K_n(k_2 R_1) I'_n(k_2 R_2)] \times \\ [J_n(k_3 R_3) Y_n(k_3 R_2) - J_n(k_3 R_2) Y_n(k_3 R_3)], \quad (4)$$

where  $k_1 = [(2m_1^*/\hbar^2)E_{nl}]^{1/2}$ ,  $k_2 = [(2m_2^*/\hbar^2)(U_B - E_{nl})]^{1/2}$ ,  $k_3 = [(2m_3^*/\hbar^2)E_{nl}]^{1/2}$ ;  $m_i^*$  ( $i = 1, 2, 3$ ) is the electron effective mass; and,  $J_n$  is the Bessel function of first kind,  $Y_n$  the Bessel function

of second kind and  $K_n, I_n$  are the modified Bessel functions<sup>15</sup>, respectively;  $f'(x) = df(x)/dx$ . In the course of deriving Eq. (3), we adopted the hard - wall model, i.e.,  $U(\rho) = 0$  for  $\rho \geq R_3$ . From the definitions and properties of Bessel functions<sup>15</sup>, it can be deduced readily that, eigenstates with nonzero azimuthal quantum number are doubly degenerate ( $E_{nl} = E_{-nl}$ ), which is the result of cylindrical symmetry of Quantum Cable. Combining Eqn. (2) with Eqn. (3), one can calculate the ballistic conductances in an accurate way. Electron's effective masses in different layers, in our calculations, are set as  $m_1^* = 5.73 \times 10^{-32}kg, m_2^* = 1.4m_1^* m_3^* = m_1^*$ , as one did in the usual  $GaAs/Ga_{0.7}Al_{0.3}As$  heterostructures.

### III. RESULTS AND DISCUSSION

For comparison, we begin with the study of ballistic conductances versus Fermi energy of single solid and hollow quantum cylinders and single 2D quantum waveguide. In Fig. 1 we give the ballistic conductances for 2D quantum waveguide, solid quantum cylinder and hollow quantum cylinder and their corresponding subband dispersions. It follows from Eqn. (2) that the ballistic conductance rises in step-like manner with the increasing Fermi energy, and that the distribution of the conductance steps is determined by the transverse mode energy  $E_{nl}$ . For 2D quantum waveguide structure, electronic states in the channel are characterized by only one quantum number  $n$ , and, the transverse energy is given by  $E_n = n^2\pi^2\hbar^2/(2m_1^*a^2)(n = 1, 2, 3, \dots)$ , where  $a$  is the width of the waveguide. Then conductance would increase a quantum conductance unit  $2e^2/h$  each time Fermi energy goes across a transverse subband; the step width increases with the increment of Fermi energy and is decided by the energy difference between neighboring subbands. The step-fashioned conductance vs Fermi energy was plotted in Fig. 1 (a) for single 2D quantum waveguide of width 210 nm. In the cases of 3D cylindrical quantum wire structure, because of the azimuthal degeneration of the transverse modes (electrons with azimuthal quantum number  $n$  and  $-n$  have the same transverse momenta) steps of one ( $n = 0$ ) or two quantum conductance units ( $n \neq 0$ ) can be observed. While the steps of two quantum conductance units can only be expected in the weakly-coupling two 2D quantum waveguides at low Fermi energies due to the twofold degeneracy of lowest subband energy dispersions. To verify this, we plotted the ballistic conductance for single solid quantum cylinder of radius 60 nm in Fig. 1 (b), and that for single hollow quantum cylinder of inner radius 100 nm and outer radius 150 nm in Fig. 1 (c). It is evident that, steps of one

or two quantum conductance units appeared. We also noticed that nonuniform distribution of conductance step width for solid cylinder; similar plateau-like structure as the 2D waveguide exists in the ballistic conductance of hollow cylinder within consecutive energy domains. This feature can be understood from the subband spectrum of hollow cylinder, since its energy difference between transverse subbands belong to the same azimuthal quantum number  $n$  will be increased with the increase of the radial quantum number  $l$  in the similar way as 2D quantum waveguide's, while that between states of the different azimuthal quantum number  $n$  is comparatively large, thus one can observed its similar step-like conductance structure within consecutive energy regions as that in 2D waveguide case.

As a solid quantum cylinder is coupled with a hollow cylinder through a tunable barrier, Quantum Cable structure is formed. It is therefore expected that coupling effects would be reflected in the ballistic conductance profile. Fig. 3 presents the calculation results of ballistic conductance vs Fermi energy of Quantum Cable with structure parameters  $R_1 = 30$  nm,  $R_3 - R_2 = 30$  nm,  $U_B = 20$  meV for variational barrier width  $R_B$ . With the increase of barrier width, that is to say, as the coupling between two cylinder wires becomes weak, more narrower conductance plateaus are displayed, some of conductance plateaus tend to be narrower while some becomes broader; some other becomes narrower first and then broader. This individuality originates also from the unique subband structure of Quantum Cable, energy spacing between consecutive subbands varies inhomogeneously with the broadness of the coupling barrier, as shown in our previous work<sup>13</sup>. In the extreme limit (i.e.,  $R_B \rightarrow \infty$  or  $U_B \rightarrow \infty$ ), Quantum Cable turns into the uncoupled cylinders structure. Then ballistic conductance spectrum is simply determined by the crude arrangement of subbands of solid and hollow quantum cylinders, and will show conductance characters of both solid and hollow cylindrical wires, which can be easily found in the  $R_B = 20$  nm case. Another observable phenomenon is the gathering of conductance steps within Fermi energy 4 – 7 meV due to the subband bundling effects<sup>13</sup> for the weakening of the coupling between two cylinders. It should be noticed that, steps of three and four quantum conductance units can also be expected to be observed (see, for example,  $R_B = 8$  nm case and  $U_B = 35$  meV case in Fig. 4). This feature stems from the accidental degeneracies (crossings) of transverse modes caused by some kind of symmetry. Since the subband (0,0) keeps the ground subband albeit of Cable structure parameters, and the subband (0,1) tends to be the first excited subband as the coupling becomes weak enough, thus one

can find that the height of first conductance step is always  $2e^2/h$ , and that of the second will be also one quantum conductance unit as the coupling is weak enough; in other words, the steps of one quantum conductance unit tend toward low Fermi energy region as the barrier width increases.

An alternative way to change the coupling strength between two wires is that the variation of coupling barrier height. In Fig. 4 we give the conductances for different barrier height from 0 to 40 meV. As in the case of increased barrier width, ballistic conductances for lifted barrier height show similar features, except that, the total number of conductance plateaus increases in the former case while it is reduced in the later case. The reason is that the energies of most subbands tend to decrease for increasing width but increase for raising barrier height, as shown in the Cable subband spectrum in both cases<sup>13</sup>.

In general, conductance plateaus of very narrow width or steps of two quantum conductance units are expected for the 2D weakly coupled quantum waveguides with two same width waveguides, and they will be violated by the deviation of the width of one of the waveguides. Since, for such structure, crossing occurs between two states with the same symmetry<sup>16</sup>, then if the widths of the two waveguides are not the same, its defining potential will be clearly asymmetric and thus its eigensubbands do not exhibit subband crossings. However, plateaus of narrower width or of three or four quantum conductance units can be observed in the Quantum Cable of cylinders with different radius. For Quantum Cable structure, subband crossings is foreign to the parameters associated with cylinders radii. In Fig. 5, conductances as a function of Fermi energy are plotted for different outer cylinder radius  $R_1$ , where  $R_B = 5$  nm,  $R_3 - R_2 = 30$  nm,  $U_B = 20$  meV. Although one does not see the steps of three or four conductance units, they can be assured to exist in the case of  $R_1$  being near 31 nm from the conductance curves for  $R_1 = 30, 31, 32$  nm, or directly from the relation of subband energy with the inner cylinder radius<sup>13</sup>. In addition, one can notice that the second step of only one quantum conductance unit may not always move to abut against the first step of one conductance unit. We then can conclude that conductance steps of one quantum conductance unit  $2e^2/h$  appear as the first and second steps only if the cylindrical wires of Quantum Cable are of the same width.

#### IV. CONCLUSIONS

In this paper, we studied ballistic electronic transport in Quantum Cable formed by a solid

cylinder, hollow cylinder and a cylindrical coupling potential barrier. Because of the azimuthal degeneration of the transverse modes (electrons with azimuthal quantum number  $n$  and  $-n$  have the same transverse momenta), steps of one or two quantum conductance units can be observed in solid and hollow quantum cylinders; while in 2D quantum waveguide, steps of one quantum conductance unit can only be expected. Since Quantum Cable is constructed by a solid and a hollow quantum cylinder which are coupled by a tunable potential barrier, apart from the above features, conductance will displays some properties originated from the coupling effects. As one of two cylinder widths or the width or height of the coupling barrier is varied, conductance plateaus of more than two quantum conductance units could be seen, due to the fact that transverse modes will cross for some parameters. Arising from the inhomogeneous variation of energy difference between adjoining subbands, some ballistic conductance plateaus exhibit oscillation. One plateau with conductance height of  $2e^2/h$  is always the first conductance step irrespective of parameter values, since the transverse mode  $(0,0)$  keeps the ground subband whatever the value of structure parameters. As the coupling between two cylinders of the same width becomes weak, i.e., the width or height of barrier increases, the other step of only one quantum conductance unit  $2e^2/h$  shifts into the second ballistic conductance step. This phenomenon can also be explained from the subband spectrum of Quantum Cable.

## ACKNOWLEDGEMENT

This work is supported by a key project for fundamental research in the National Climbing Program of China.

## References

‡ E-mail address: zyzeng@mail.issp.ac.cn

1. H. Van Houten, C. W. J. Beenakker, and B. J. von Wees, *Semicond. Semimet.* **35**, 9 (1992).
2. J. A. Torres, J. I. Pascual, and J. J. Saenz, *Phys. Rev. B* **49**, 16581 (1994); A. G. Scherbakov, E. N. Bogachek, and Uzi Landman, *ibid.* **53**, 4054 (1996).
3. G. Kirczenow, *Solid State Commun.* **68**,715 (1988); A. Szafer and A. D. Stone, *Phys. REv. Lett.* **62**, 300 (1989); N. Garcia and L. Escapa, *Appl. Phys. Lett.* **54**, 1418 (1989); E. G.

- Haanappel and D. van der Marel, Phys. Rev. B **39** 5484 (1989); A. Matulis and D. Segzda, J. Phys. Condens. Matter **1**, 2289 (1989); M. Yosefin and M. Kaveh, Phys. Rev. Lett. **64**, 2819 (1990); E. Tekman and S. Ciraci, Phys. Rev. B **43**, 7145 (1991).
4. R. Landauer, Philos. Mag. **21**, 863 (1970); M. Büttiker, Phys. Rev. Lett. **57**, 1761 (1986).
  5. S. Datta and M. J. McLennan, Rep. Prog. Phys. **53**, 1003 (1990); T. J. Thornton, *ibid.* **57**, 311 (1994).
  6. F. Sols, M. Macucci, U. Ravaioli, and K. Hess, Appl. Phys. Lett. **54**, 350 (1989); Y. Avishai and Y. B. Band, Phys. Rev. B **41**, 3253 (1990); J. Wang, Y. J. Wang, and H. Guo, *ibid.* **46**, 2420 (1992); Z. -L. Ji and K. -F. Berggren, *ibid.* **45**, 4662 (1992); H. Xu, *ibid.* **47**, 9537 (1993); H. U. Baranger and P. A. Mello, Phys. Rev. Lett. **73**, 142 (1994).
  7. Mesoscopic Phenomena in Solids, edited by B. L. Altshuler, P.A. Lee and R. A. Webb, (Elsevier Science Publishers B. V. ) (1991).
  8. S. Luryi and F. Capasso, Appl. Phys. Lett. **47**, 1347 (1985); S. Datta, M. R. Melloch, S. Bandyopadhyay, R. Noren, M. Vaziri, M. Miller, and R. Reifenberger, Phys. Rev. Lett. **55**, 2344 (1985); T. J. Thornton, M. Pepper, H. Ahmed, D. Andrews, and G. J. Davies, Phys. Rev. Lett. **56**, 1198 (1986); K. Tsubaki and Y. Tokura, Appl. Phys. Lett. **53**, 859 (1989); R. Q. Yang and J. M. Xu, Phys. Rev. B **43**, 1699 (1991).
  9. J. A. del Alamo and C. C. Eugster, Appl. Phys. Lett. **56**, 78 (1990); Phys. Rev. Lett. **67**, 3586 (1991).
  10. C. C. Eugster, J. A. del Alamo, M. J. Rooks, and M. R. Melloch, Appl. Phys. Lett. **60**, 642 (1992); C. C. Eugster, J. A. del Alamo, M. R. Melloch, and M. J. Rooks, Phys. Rev. B **46**, 10406 (1992); *ibid.* **48**, 15057 (1993); J. Wang, H. Guo, and R. Harris, Appl. Phys. Lett. **59**, 3075 (1991); J. Wang, Y. J. Wang, and R. Harris, Phys. Rev. B **46**, 2420 (1992); J. R. Shi and B. Y. Gu, *ibid.* **55**, 9941 (1997).
  11. X. Suenaga, C. Colliex, N. Demoncey, A. Loiseau, H. Pascard, and F. Willaime, Science **278**, 653 (1997).
  12. Y. Zhang, K. Suenaga, C. Colliex and S. Iijima, Science **281**, 973 (1998).

13. Z. Y. Zeng, Y. Xiang, and L. D. Zhang (unpublished).
14. E. N. Bogachek, A. N. Zagoskin, and I. O. Kukik, *Fiz. Nizk. Temp.* **16**, 1404 (1990) [*Sov. J. Low. Temp. Phys.* **16**, 796 (1990)].
15. *Handbook of Mathematical Functions*, edited by M. Abramowitz and I. A. Stegun (New York, Dover) (1972).
16. M. A. Morrison, T. L. Estle, and N. F. Lane, *Quantum States of Atoms, Molecules, and Solids* (Prentice - Hall Inc., New Jersey) (1976).

## Figure Captions

**Fig. 1** A schematic view of ballistic Quantum Cable structure, where  $R_1$  is the radius of inner solid quantum cylinder,  $R_2$  and  $R_3$  are the inner radius and outer radius of outer hollow cylinder, respectively; two cylinders are coupled through a tunable potential barrier of width  $R_B = R_2 - R_1$  and height  $U_0$ .

**Fig. 2** Conductance as a function of Fermi energy and the corresponding energy dispersion for (a) 2D quantum waveguide of width 210 nm, (b) solid quantum cylinder of radius 60 nm and (c) hollow quantum cylinder of inner radius  $R_2 = 100$  nm and outer radius  $R_3 = 150$  nm.

**Fig. 3** Conductance of Quantum Cable as a function of Fermi energy for different barrier width  $R_B$ , where structure parameters are chosen such that  $R_1 = 30$  nm,  $R_3 - R_2 = 30$  nm,  $U_B = 20$  meV.

**Fig. 4** Conductance of Quantum Cable as a function of Fermi energy for different barrier height  $U_B$ , where structure parameters are chosen such that  $R_1 = 30$  nm,  $R_3 - R_2 = 30$  nm,  $U_B = 5$  meV.

**Fig. 5** Conductance of Quantum Cable as a function of Fermi energy for different solid cylinder radius  $R_1$ , where structure parameters are chosen such that  $R_B = 5$  nm,  $R_3 - R_2 = 30$  nm,  $U_B = 20$  meV.

Fig.1 Zeng et al.

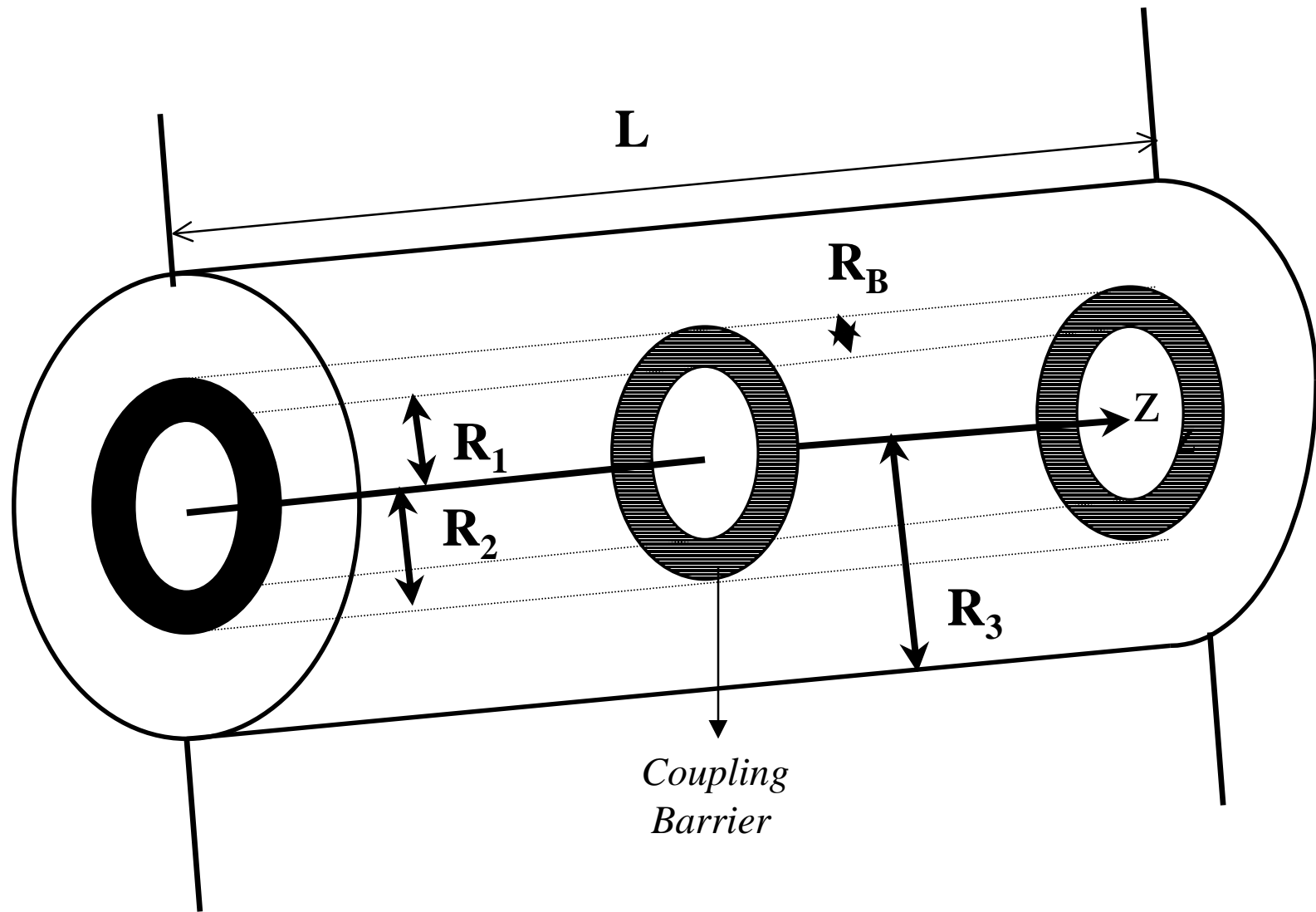


Fig. 2 Zeng et al.

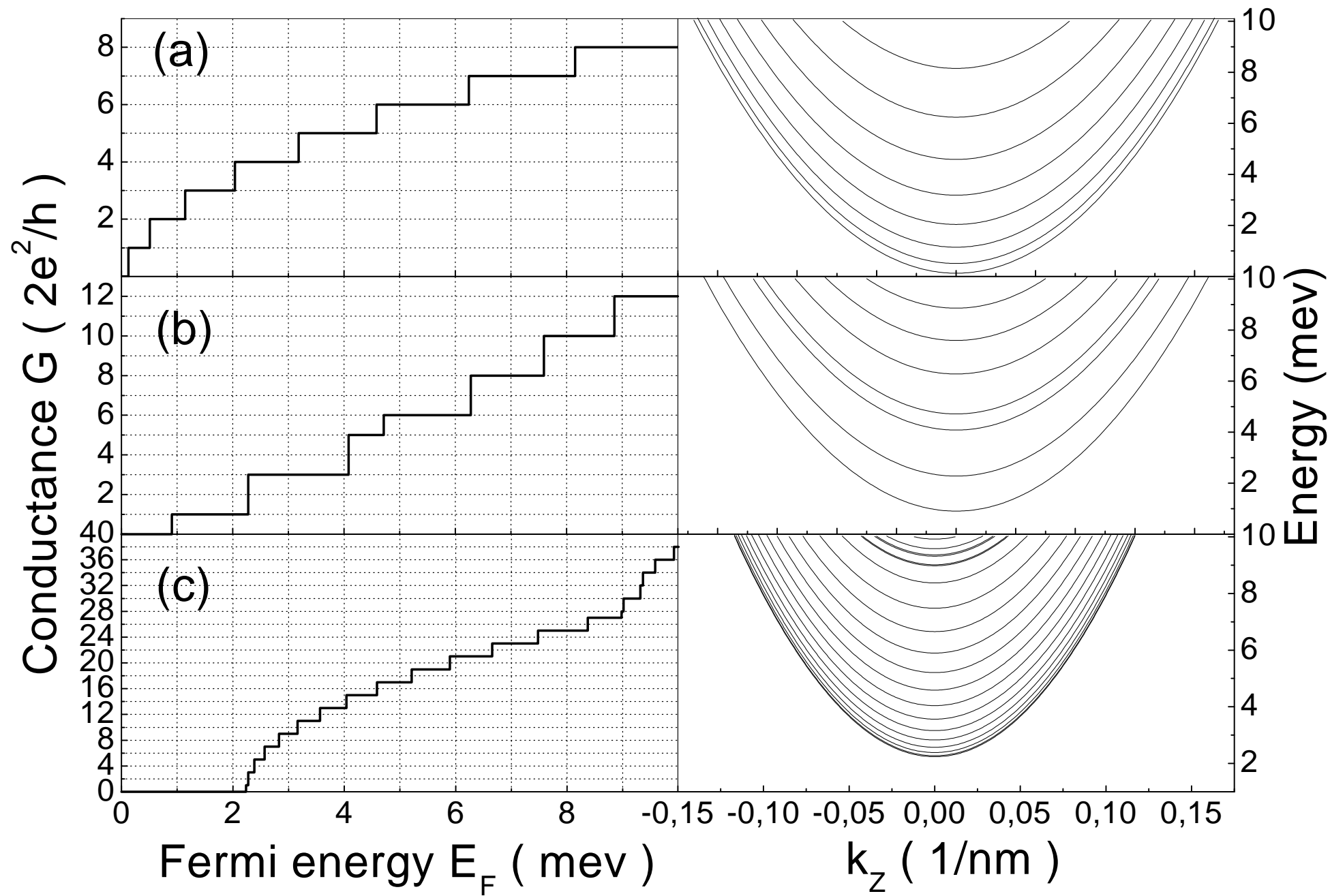


Fig. 3 Zeng et al.

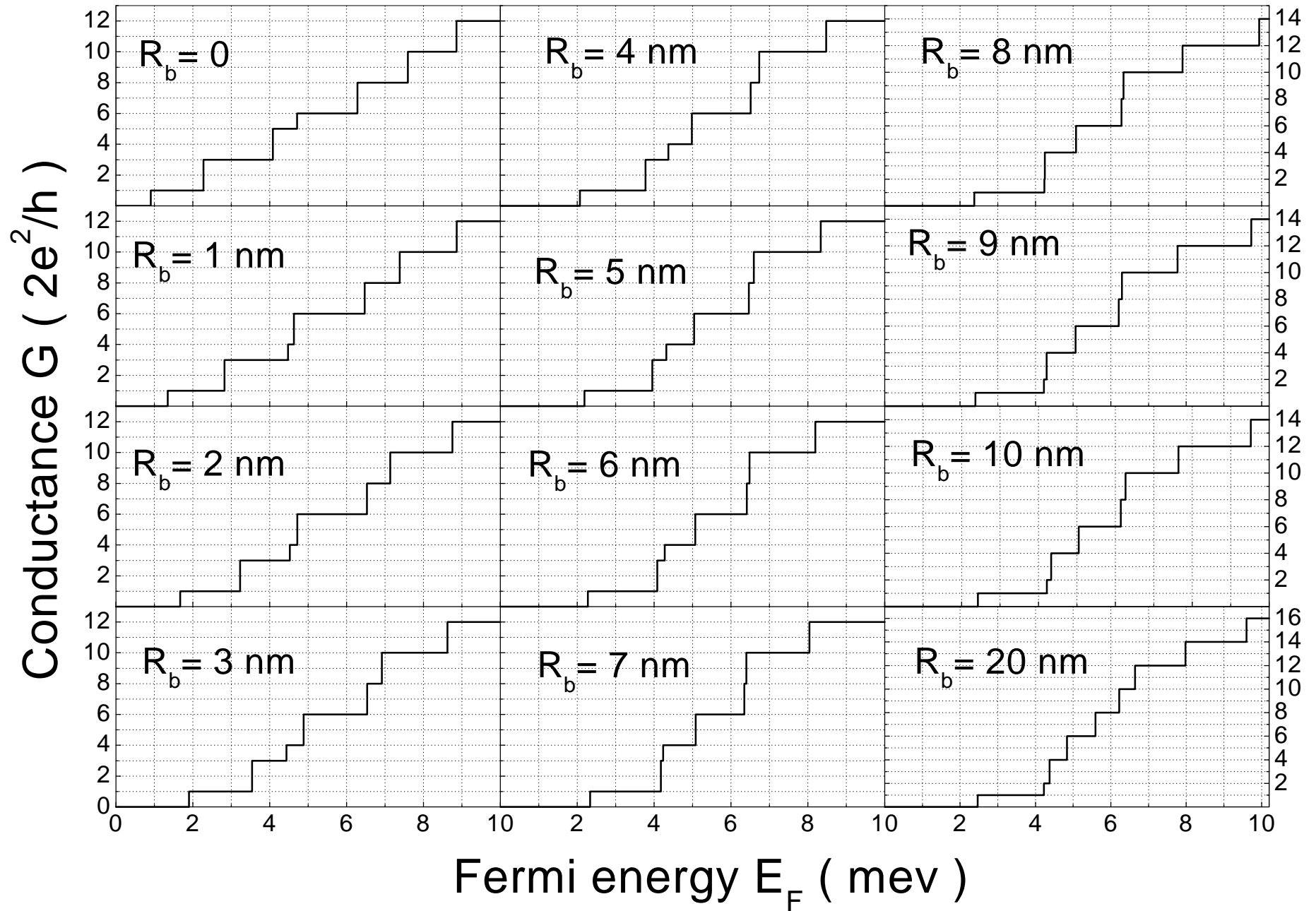


Fig. 4 Zeng et al.

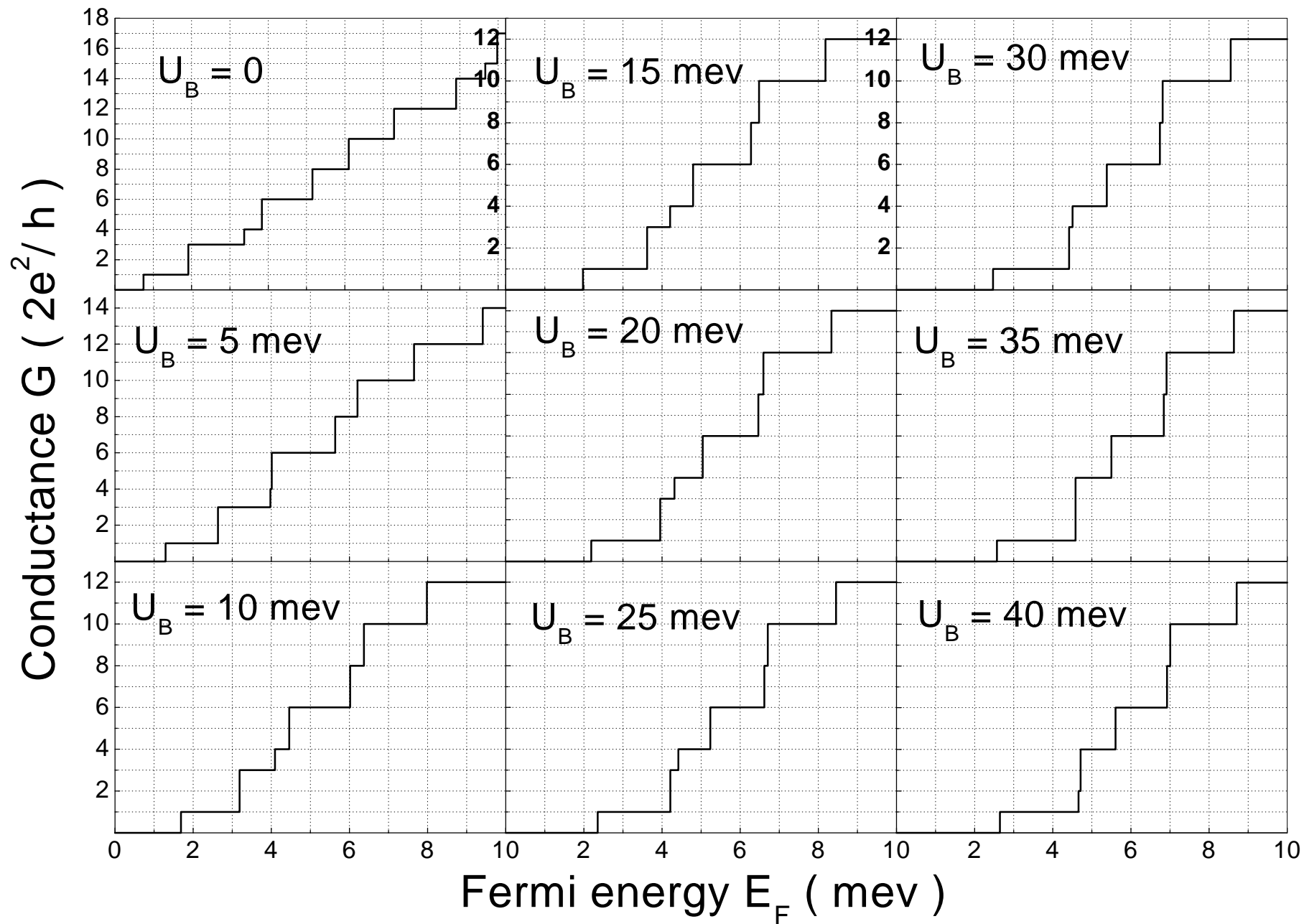


Fig. 5 Zeng et al.

